

THERMOGRAVIMETRY AS A METHOD FOR INVESTIGATING THE THERMAL STABILITY OF POLYMER COMPOSITES

A. T. Ponomarenko, C. Klason¹, N. E. Kazantseva, M. I. Buzin², M. Alexandre³, Ph. Dubois³, I. A. Tchmutin, V. G. Shevchenko and R. Jérôme³

Enikolopov N. S. Institute of Synthetic Polymeric Materials, Russian Academy of Science Moscow, Russia

¹Department of Polymeric Materials, Chalmers University of Technology, Gothenburg, Sweden

²Institute of Organoelement Compounds, Russian Academy of Science, Moscow, Russia

³Center for Education and Research on Macromolecules, University of Liège, Belgium

Abstract

Thermogravimetry was used to investigate the effects of different inorganic functional fillers on the heat resistance of polymer matrices. The kinetic parameters of thermal oxidative degradation were shown to depend on the polymer, the chemical composition of the filler surface, the filler concentration, and the processing method, which determines the distribution of filler particles in the polymer matrix. Magnetic fillers (carbonyl iron, and hexaferrites of different structural types) were shown to be chemically active fillers, increasing the heat resistance of siliconorganic polymers. Their stabilizing effect is due to blocking of the end silanol groups and macroradicals by the surface of the filler and non-chain inhibition of thermal oxidative degradation. In the case of fiber-forming polymers (UHMWPE, PVOH and PAN), most magnetic fillers are chemically inert, but at concentrations of 30–50 vol% they increase the heat resistance of the composite. Addition of carbon black increased the heat resistance of the thermoplastic matrix. The dependence of the thermal degradation onset temperature on the kaolin concentration in the polyolefin matrix exhibited a maximum. Analysis of the experimental results demonstrated the operating temperature ranges for different composites, and their maximum operating temperature.

Keywords: functional fillers, polymer composite, thermogravimetry

Introduction

Investigations relating to the effects of different fields, including thermal ones, on polymer composites is important from the following aspects: the selection of ingredients of composites, the engineering technologies for new materials and structures with necessary sets of properties, and forecasting of the dynamics of these properties. For this reason, thermal spectroscopy, as one of the branches of materials science, occupies a special position in investigations aimed

at the improvement of materials in such modern technologies as those involving smart materials and structures, microelectronics, electrical engineering, etc. [1, 2].

The analysis of thermal curves (DTA, DTG and TG) of ingredients and composites can reveal the intervals of their thermal stability in air and inert atmospheres, and permit evaluations of the effects of fillers in thermal and oxidative degradation, which in turn allows the specification of temperature conditions of processing and use.

The purpose of the work reported here was to obtain initial data on the thermal stabilities of polymers of various classes and composite materials obtained by the introduction into these polymers of functional fillers, and to determine the directions of subsequent more detailed investigations.

Experimental

Sample preparation

1. As conducting filler, carbon black (CB) Printex XE-2 (from Degussa) was used. The polymer matrix was HDPE (Eltex B 3925 from Solvay, $MW=265\ 000$ and crystallinity 50%), or a mixture of this polyethylene (PE) with polystyrene (PS) (158 K from BASF, $MW=280\ 000$).

Three series of composites were prepared. It has previously been shown that different matrices and mixing techniques result in different localizations of the filler [3, 4]:

- a) CB was dispersed in an amorphous phase of PE;
- b) CB was dispersed in the PE phase of a cocontinuous PE/PS blend of 45/55 mass% composition;
- c) CB was localized at the interface of a cocontinuous PE/PS blend of 45/55 mass% composition.

2. Epoxy resin AT1 (CIBA-GEIGY AB, Sweden) in powder form was used as dielectric matrix. The ferroelectric filler was barium titanate ($BaTiO_3$) (Novakemi AB, Sweden), its particles having a typical size of 1.8 μm . The conducting filler was CB (Vulcan XC-72 from Cabot) with an average particle size of 30 nm. The volume fraction of $BaTiO_3$ in the composite (v_{BaTiO_3}) was varied from 0 to 56 vol% with the CB concentration varying from 0 to 12 vol%.

During preparation of the samples, the components of the composites were mixed in powder form in a Retsch MM2 shaker at room temperature and then compression-molded at 180°C. After compression-molding, the samples were postcured at 180°C.

3. Composites with PE were made by mixing the components in a Brabender mixer at a temperature above T_{melt} of PE and subsequent pressure-molding. The volume fraction of $BaTiO_3$ in the composite (v_{BaTiO_3}) was varied from 0 to 56 vol%, with the CB concentration (v_{CB}) varying from 0 to 10 vol%.

4. The fibers were gel-spun from UHMWPE and hexagonal ferrite (hexaferrite) and amorphous alloy fillers with a particle size of 150–400 μ and a filler volume fraction up to 60%. Just-drawn fibers are considerably porous and possess a rather low tensile strength. The influence of additional deformations at elevated temperature on the magnetic texture and on the electrodynamic and mechanical properties of the fibers was investigated. During this treatment, ferrite particles become oriented in the polymer matrix, with the vector of the magnetic moment assuming a preferential direction, either in the plane of the fiber or normal to it, so that the fibers become magnetically textured. Measurements of electrodynamic properties in the frequency range 4–40 GHz reveal that textured structures are superior to isotropic ones in this respect.

5. The fibers were drawn from ftorlon (a copolymer of tetrafluoroethylene and vinylidene fluoride with a molecular mass of $2.2 \cdot 10^5$), filled with powders of magnetically soft hexagonal ferrites and carbonyl iron. The hexaferrite particles had an anisotropic shape and were 100 μ in size, while the iron particles were spherical and 2–8 μ in diameter. The volume fraction of the filler v_f was up to 60%.

6. Polyethylene–kaolin composites were prepared by using a polymerization-filling technique by ethylene polymerization with Al/Ti/Mg catalyst previously deposited on the surface of the filler particles. Kaolin (Satintone W/W) was previously heated overnight at 100°C at 10^{-2} mm Hg. The contents of hydroxyl groups and adsorbed water were titrated volumetrically. The catalyst was attached onto the filler in such a way that either 50 or 25% of the kaolin OH groups were consumed. Ethylene was polymerized in a batch mode at 60°C in a 2 L stainless steel Autoclave Engineers reactor equipped with a magnetic coupled stirrer with a variable stirring speed and an external jacket heater. The addition of a transfer agent such as hydrogen has proved to lead to efficient control of the matrix molecular mass.

7. Liquid perfluoroethers with functional groups are transparent liquids with a viscosity of 30 poise at 25°C. As a curing agent, xylenediamine can be used at a concentration of 6.5–7% relative to the polymer mass. The composition is prepared by mixing the liquid polymer, filler and curing agent immediately before use, followed by curing at room temperature during 1 h. For optimum mechanical properties, the following regime is necessary: 24 h at room temperature and 24 h at 60–80°C (minimum 12 h at 70°C).

8. Polyorganosilsesquioxanes (industrial name Lestosil-SM), which are polymer powders with a particle size of 500–1000 μ , readily soluble in organic solvents such as toluene, benzene, acetone, chloroform, butyl acetate, etc., were used as polymeric matrix for composites with a magnetic filler. As 'cold' cure catalytic system, the following can be used: a solution of tin diethyldicaprylate in tetraethoxysilane in 1:4 ratio; a solution of tin diethyldilaurylate in tetraethoxysilane in 1:1 ratio; methyltriacetoxylane; or vinylloxime, $\text{CH}_2=\text{CH}-\text{Si}[\text{ON}=\text{C}(\text{CH}_3)_2]_3$. In the processing of composites from Lestosil-SM, the solvent, the catalytic system and the concentration of the poly-

mer were varied. The composition was prepared by mixing liquid polymer, filler and curing agent immediately before use.

Results and discussion

An analysis of the data in Table 1 permits the general conclusion that such fillers as iron, ferrites and amorphous alloys can exhibit similar chemical effects in the thermal oxidative degradation of polymer matrices [6–9], but in each particular case the results need additional analysis.

Table 1 Chemical inhomogeneity of composition of the surface of carbonyl iron, ferrites and amorphous alloys from X-ray photoelectron spectroscopy data

No.	Filler	Chemical composition of the surface	Nature of chemical inhomogeneity of filler surface	Active centers
1.	Carbonyl iron R-10, R-20	FeO, Fe ₂ O ₃ , Fe ₃ C, Fe ₄ N, Fe ⁰ , Fe(OH) ₂	Lewis acid Brönstead centers	L ₁ ⁺ , L ₂ ⁺ , L ₂₁ ⁺ B ₁ , B ₂
2.	Carbonyl iron whiskers, RC00227	FeO, Fe ₂ O ₃ , Fe ₃ C, Fe ₄ N, Fe(OH) ₂	Lewis acid Brönstead centers	L ₁ ⁺ , L ₂ ⁺ , L ₂₁ ⁺ B ₁ , B ₂
3.	Hexagonal ferrites BaFe _{12-x} M _x O ₁₉			
3.1.	M=Ti ⁴⁺ , Co ²⁺	FeO, BaO, TiO ₂	Lewis acid Brönstead centers	L ₁ ⁺ , L ₂ ⁺ , L ₂₁ ⁺ B ₁ , B ₂
3.2.	Ni ₂ W, doped with Sc e.g. Ni ₂ BaSc _{0.2} Fe _{15.8} O ₂₇	FeO, Sc ₂ O ₃	Lewis acid Brönstead centers	L ₁ ⁺ , L ₂ ⁺ , L ₂₁ ⁺ B ₁ , B ₂
3.3.	Ba 0.6(Zn, Zr) 0.1Mn5.2Fe ₂ O ₃	FeO, Fe ₂ O ₃ , ZnO, MnO, Mn ₂ O ₃ , MnO ₂ , BaO	Lewis acid Brönstead centers	L ₁ ⁺ , L ₂ ⁺ , L ₂₁ ⁺ B ₁ , B ₂
3.4.	Ni ₂ SrFe ₁₆ O ₂₇	FeO, NiO, SrO	Lewis acid	L ₁ ⁺ , L ₂ ⁺ , L ₂₁ ⁺
3.5.	Ni ₂ SrCr _{0.8} Fe _{15.2} O ₂₇	Fe ₂ O ₃ , SrO, Cr ₂ O ₃	Lewis acid	L ₁ ⁺ , L ₂ ⁺ , L ₂₁ ⁺
4.	Amorphous alloys			
4.1.	Fe-Si-B 71KNSP	FeO, NiO, SiO ₂ , MnO, CoO	Lewis acid	L ₁ ⁺ , L ₂ ⁺ , L ₂₁ ⁺
4.2.	Fe-Si-B P82K3XCP	FeO, CuO, PbO, MgO, SiO ₂	Lewis acid	L ₁ ⁺ , L ₂ ⁺ , L ₂₁ ⁺

L₁⁺ – regular lattice cations, L₂⁺ – anion vacancies, L₂₁⁺ – local surface regions with oxygen vacancies and partially reduced metal cations;

B₁ – Brönstead bases, B₂ – Brönstead acids

Carbon black-filled composites

Table 2 and Fig. 1 show that the presence of even 1% of CB in composites of type 1a markedly increases the thermal oxidation stability of PE. The melting temperature remains the same, whereas the temperatures of the onset and maximum of the peak in the DTA curve (Fig. 8), related to the oxidation processes, increase by 20–25°C. This temperature shift increases with increasing CB volume fraction. Although the temperature of the beginning of oxidation decreases slightly, by 30°C, this fact is of no significance, since degradation occurs at a much higher temperature than the operating temperature range of these composites.

Table 2 and Figs 2 and 3 reveal that the mixing method and the distribution of the filler have marked effects on the thermal properties of composites of types 1b

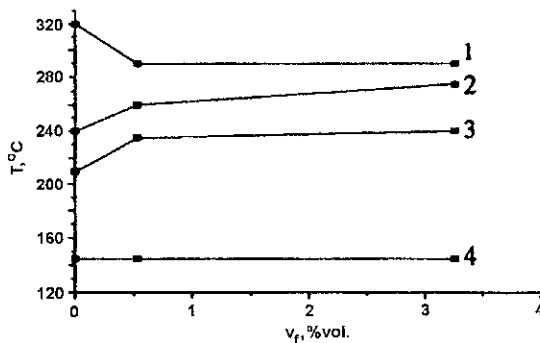


Fig. 1 Dependence of the 2% mass loss temperature $T_g^{2\%}$ (1), the temperature of maximum oxidation rate $T_{\text{ox,max}}$ (2), the temperature of oxidation beginning $T_{\text{ox,begin}}$ (3) and the melting temperature T_{melt} (4) on the volume fraction of CB for PE-CB composites of type 1a

Table 2 Parameters of thermal-oxidative degradation* of carbon black-filled composites with different localizations of filler particles

Composition	$T_{\text{melt}}, ^\circ\text{C}$	$T_{\text{ox,begin}}, ^\circ\text{C}$	$T_{\text{ox,max}}, ^\circ\text{C}$	$T_g^{2\%}, ^\circ\text{C}$
PE	145	210	240	320
PE + CB 1 vol%	145	235	260	290
PE + CB 6 vol%	145	240	275	290
PE/PS	135	200	225	320
PE/PS + CB (CB in PE) 1 vol%	135	200	225	330
PE/PS + CB (CB in interphase) 0.5 vol%	135	220	240	280
PE/PS + CB (CB in interphase) 1 vol%	110	220	240	350

* Thermal properties of composites and ingredients were investigated in the temperature interval between 25°C and the temperature of the end of degradation T^f with a MOM Derivatograph-C (in air) and in some cases with a Setaram B-60 analyser (in argon) at a temperature increase rate of 10°C min⁻¹

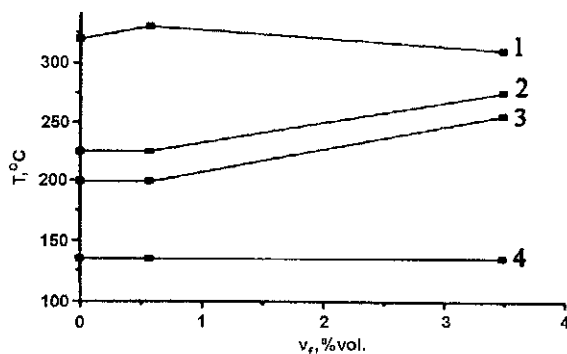


Fig. 2 Dependence of the 2% mass loss temperature $T_{\xi}^{2\%}$ (1), the temperature of maximum oxidation rate $T_{ox,max}$ (2), the temperature of oxidation beginning $T_{ox,begin}$ (3) and the melting temperature T_{melt} (4) on the volume fraction of CB for PE/PS-CB composites; CB is dispersed in PE phase of type 1b

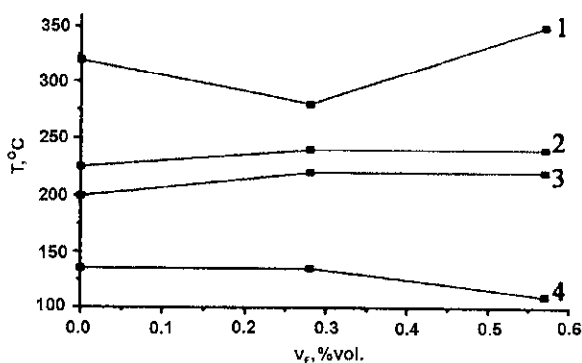


Fig. 3 Dependence of the 2% mass loss temperature $T_{\xi}^{2\%}$ (1), the temperature of maximum oxidation rate $T_{ox,max}$ (2), the temperature of oxidation beginning $T_{ox,begin}$ (3) and the melting temperature T_{melt} (4) on the volume fraction of CB for PE/PS-CB composites; CB is dispersed in the interphase PE/PS of type 1c

and 1c. Similarly as for the electrical properties, the presence of a small amount of CB dispersed in the interphase PE-PS markedly increases the thermal oxidation stability of the composites. Both $T_{ox,begin}$ and $T_{ox,max}$ increase.

Epoxy resin+carbon black+BaTiO₃

The presence of functional fillers has little effect on the service properties of the composites. The temperature of the beginning of oxidation remains practically the same (Fig. 4). Comparison of the TG and DTA data demonstrates that the initial stage of degradation corresponds to oxidation processes. It is clear from Fig. 4 that the amplitude and position of the exo-peak in the DTA curve de-

pend on the nature and the amount of the functional filler. However, these changes occur in the temperature range of degradation and their effect is not significant.

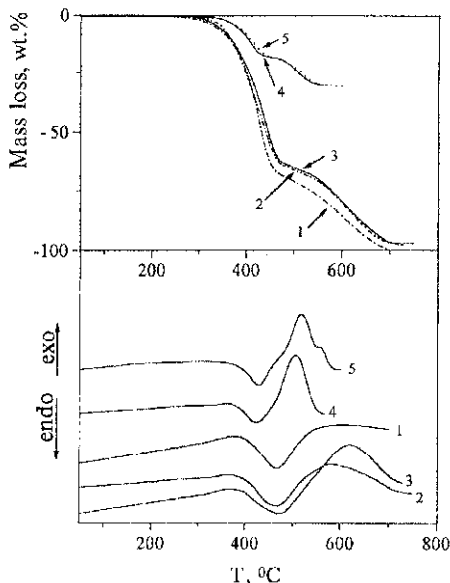


Fig. 4 TG and DTA curves for 1 – epoxy resin and composites; 2 – epoxy resin–CB (3.9 vol%); 3 – epoxy resin–CB (4.6 vol%); 4 – epoxy resin–barium titanate (35 vol%) + CB (3.5 vol%); 5 – epoxy resin–barium titanate (35 vol%)+CB (5.5 vol%)

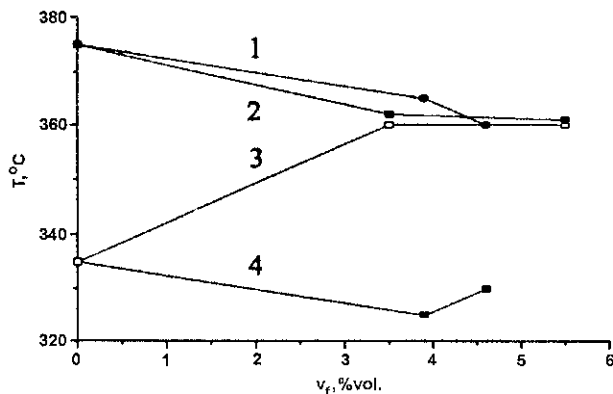


Fig. 5 Dependence of the temperature of maximum oxidation rate $T_{ox,max}$ (1, 2), and the 2% mass loss temperature $T_g^{2\%}$ (3, 4), on the volume fraction of CB for epoxy resin–CB composites (1, 4) and epoxy resin–CB–barium titanate composites (2, 3)

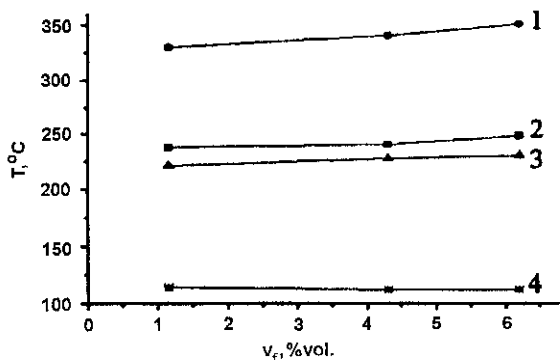


Fig. 6 Dependence of the 2% mass loss temperature $T_{2\%}$ (1), the temperature of maximum oxidation rate $T_{ox,max}$ (2), the temperature of oxidation beginning $T_{ox,begin}$ (3) and the melting temperature T_{melt} (4) on the volume fraction of CB for PE-CB composites

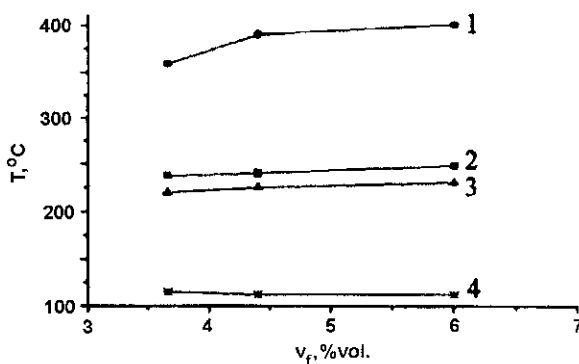


Fig. 7 Dependence of the 2% mass loss temperature $T_{2\%}$ (1), the temperature of maximum oxidation rate $T_{ox,max}$ (2), the temperature of oxidation beginning $T_{ox,begin}$ (3) and the melting temperature T_{melt} (4) on the volume fraction of CB for PE-CB-barium titanate composites

Polyethylene+carbon black+BaTiO₃

As the data in Figs 6 and 7 show, an increase of the CB content increases the thermal and thermal oxidation stabilities of the composites. Both the temperature of thermal oxidation and the temperature of degradation shift to higher values.

UHMWHE with magnetic fillers

Fibers from UHMWPE and magnetic fillers have different thermal stabilities. Table 3 presents parameters relating to the thermal oxidative degradation of these fibers.

Table 3 Thermal oxidative stabilities of fibers from UHMWPE and magnetic fillers

No.	Filler	Concentration/ vol%	$T_{\text{ox.begin}}/$ $^{\circ}\text{C}$	Mass loss at $500^{\circ}\text{C}/\%$
1.	Unfilled UHMWPE	—	304.5	85
2a.	Carbonyl iron R-20	6	350	33
2b.	Carbonyl iron R-20	20	349	25
2c.	Carbonyl iron R-20	54	408	9.1
3.	Hexaferrite Co_2Z	55	287	12
4.	Mixture of hexagonal W-type ferrites	70	346.5	3.7
	$\text{Ni}_2\text{BaSc}_{0.8}\text{Fe}_{15.2}\text{O}_{27}$			
	$\text{Ni}_2\text{BaSc}_{0.4}\text{Fe}_{15.6}\text{O}_{27}$			
	$\text{Ni}_2\text{BaSc}_{0.6}\text{Fe}_{15.4}\text{O}_{27}$			

Table 4 Parameters of thermal oxidative degradation of ftorlon fibers with different magnetic powder fillers

No.	Filler	Concentration/ vol%	$T_{\text{ox.begin}}/$ $^{\circ}\text{C}$	Mass loss at $500^{\circ}\text{C}/\%$
1.	Unfilled ftorlon 42-B	—	406.7	88
2a.	Carbonyl iron R-20	20	451	26.75
2b.	Carbonyl iron R-20	60	420	2.2
2c.	Carbonyl iron "Goodfellow"	60	440	4.97
3a.	Ferrite $\text{BaFe}_{2(2-x)}\text{M}_x\text{O}_{19}$ $M=\text{Ti}^{4+}, \text{Co}^{2+}$	60	447	17.61
3b.	Mixture of hexagonal W-type ferrites*	60	353	23.64
4.	Amorphous alloy 71KNPS	60	404	9.7

* $\text{Ni}_2\text{BaSc}_{0.8}\text{Fe}_{15.2}\text{O}_{27}$, $\text{Ni}_2\text{BaSc}_{0.4}\text{Fe}_{15.6}\text{O}_{27}$, $\text{Ni}_2\text{BaSc}_{0.6}\text{Fe}_{15.4}\text{O}_{27}$

Table 3 shows that the thermal stability of UHMWPE increases in the presence of carbonyl iron. The temperature of the beginning of decomposition shifts to higher temperature, with a simultaneous increase in the induction period. The inhibiting effect of iron is explained by the formation of polymeric structures incorporating iron particles. This effect is believed to be caused not only by the changes in the UHMWPE structure (the formation of metal-polymer bonds of iron carboxylate type, and the structurization of the polymer), but also by the dissipation of the thermal energy localized on the macromolecule.

The changes in thermal stability of ferrite-filled UHMWPE fibers are related to the presence of active centers on the surface of the ferrite particles (Table 1). For example, in the case of mixed W-type ferrite as filler, both the temperature of the beginning of decomposition and the induction period increase. At the same time, the presence of hexaferrite Co_2Z decreases the thermal stability of UHMWPE fibers insignificantly.

Ftorlon with magnetic fillers

The thermal oxidative degradation of magnetic fibers from ftorlon and magnetic fillers was investigated by dynamic thermogravimetric analysis (DTG) at a heating rate of $10^\circ\text{C min}^{-1}$. The results reveal that all the kinetic parameters depend on the type of filler and its concentration in the polymer matrix (Table 4).

The DTG data on ftorlon fibers containing carbonyl iron of different types demonstrate that for the filled fibers the characteristic points of thermal oxidative degradation (beginning, end and half-disintegration temperatures) shift to higher temperatures with the appearance of the exothermic peak (423°C) due to the oxidation of carbonyl iron. These results mean that carbonyl iron inhibits the thermal oxidative degradation of ftorlon. Carbonyl iron acts as a stabilizer by deactivating oxygen and probably inhibiting thermal oxidative radical reactions.

Increased characteristic temperatures are observed for fibers containing $\text{BaFe}_{12-x}\text{M}_x\text{O}_{19}$ ($M=\text{Ti}^{4+}, \text{Co}^{2+}$), probably due to the presence of TiO_2 on the surface of this ferrite. Surface acid centers of TiO_2 promote cleavage of the C–F bond, thereby increasing the induction period for dehydrofluorination.

Other types of fillers may be regarded as inactive. Their presence does not appreciably affect the thermal stability of filled ftorlon fibers.

Composites of polyethylene-kaolin

As Table 5 and Fig. 8 show, the presence of 17.8 mass% of kaolin markedly increases the thermal oxidation stabilities of the composites. The melting temperature remains the same, while the temperatures of the onset and maximum of the peak in the DTA curve (Fig. 8) related to the oxidation processes markedly increase. Increase of the kaolin concentration to 33.5 mass% results in decreases in these parameters.

Table 5 Parameters of thermal oxidative degradation for PE and PE–kaolin composites

Composition	$T_{\text{melt}}/^\circ\text{C}$	$T_{\text{ox.begin}}/^\circ\text{C}$	$T_{\text{ox.max}}/^\circ\text{C}$	$T_g^{2\%}/^\circ\text{C}$
PE	145	210	240	320
PE + 17.8 mass% kaolin	140	280	300	340
PE + 33.5 mass% kaolin	140	210	225	285

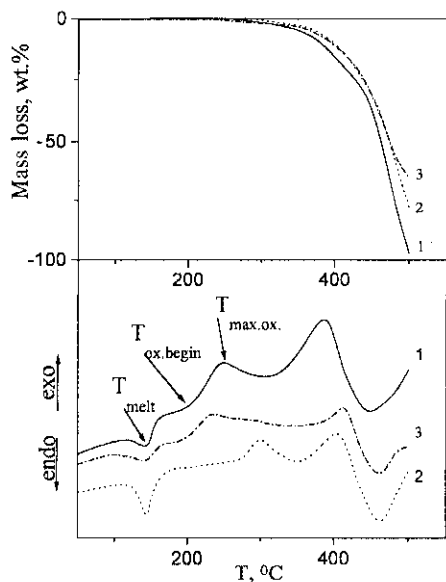


Fig. 8 TG and DTA curves for 1 – PE and composites: 2 – PE–kaolin (17.8 mass%); 3 – PE–kaolin (33.5 mass%)

Perfluoroethers with magnetic fillers

The thermal degradation of composites containing perfluoroethers with functional groups begins with the breaking of the weakest C–C bonds in the perfluoroether chain. The temperature of the onset of degradation in inert media is $\approx 410^\circ\text{C}$. Above this temperature, the macroradical decays by a chain mechanism with the formation of volatile products. The presence of aerial oxygen does not increase the rate of pyrolysis, but $T_{ox.begin}$ decreases to 310°C . Carbonyl iron has a stabilizing effect, increasing $T_{ox.begin}$ to 350°C . The presence of hexaferrites also has a stabilizing effect, increasing $T_{ox.begin}$ from 300°C for the pure polymer to $330\text{--}350^\circ\text{C}$ for the filled systems, depending on the type of ferrite.

Polyorganosilsesquioxanes with magnetic fillers

The degradation of Lestosil-SM in an argon flow at a temperature increase rate of $10^\circ\text{C min}^{-1}$ exhibits an induction period, accompanied by slight changes in molecular mass. During this period, degradation occurs by depolymerization with the transfer of active centers in linear flexible polyorganosilsesquioxane blocks. After the induction period, the bonds, connecting the phenylsilsesquioxane and dimethylsiloxane blocks undergo rupture. This period corresponds to the maximum rate of degradation. The temperature of the beginning of degradation $T_{ox.begin}$ is $\approx 360^\circ\text{C}$, while the temperature of the end of degradation T^f is $\approx 400^\circ\text{C}$,

$T_{\text{ox.begin}}$ corresponding to the exothermic peak and T^{f} corresponding to the end of the endothermic effect in the DTA curve.

In air, the presence of oxygen causes oxidation, which accelerates the degradation of polyorganosilsesquioxanes: $T_{\text{ox.begin}} \approx 325^{\circ}\text{C}$.

Investigations of the thermal and thermal oxidative degradation of composites from Lestosil-SM filled with different magnetic fillers (carbonyl iron, hexaferrites with a thermally stable field of crystallographic anisotropy, such as $\text{Ni}_2\text{Ba}(\text{Sr})\text{W}$, $\text{Ni}_{2-y}\text{Zn}_y\text{BaW}$, $\text{Ni}_2\text{SrCr}_x\text{W}$, etc.) permit the following findings. Carbonyl iron with its small particles effectively stabilizes the degradation of Lestosil-SM. The induction period increases in both cases, probably in consequence of the binding of the active centers of the degradation products by carbonyl iron. In air, the primary effect of carbonyl iron is the deactivation of oxygen, as evidenced by the appearance of an exothermic peak due to the oxidation of carbonyl iron, in contrast with the situation for the pure polymer. The stabilizing effect of carbonyl iron increases: $T_{\text{ox.begin}} \approx 360^{\circ}\text{C}$ and $T^{\text{f}} = 470^{\circ}\text{C}$.

In contrast with carbonyl iron, the effects of hexaferrites on the degradation of Lestosil-SM are insignificant and they do not change the rates of thermal and thermal oxidative degradation or the characteristic temperatures.

Conclusions

1. The experimental results attained in this work demonstrate that the parameters of thermal oxidative degradation of the investigated composites depend on the chemical structure of the polymer matrix, the type and concentration of the filler and the methods of preparation of the composites which determine their structure.

2. Some types of fillers not only provide functional properties of the composites, but also shift the thermal oxidative degradation to higher temperatures, that is they act as inhibitors of the process of degradation.

3. To evaluate the influence of thermal oxidative degradation processes on the functional properties of the investigated composites, parallel research involving their temperature dependences and the material balance of the degradation products is required.

* * *

We gratefully acknowledge the collaboration of all colleagues who helped in the preparation of the samples of polymer composites. We also thank Professor P. Staszczuk, Chairman of the 27th IVMT Conference, for fruitful discussions on the subject of this paper.

References

- 1 T. Takagi, In: Proc. of the 3rd Int. Conf. Intelligent Materials, Lyon, 3–5 June 1996, SPIE 2779, p. 2.
- 2 A. T. Ponomarenko, A. V. Buts, V. G. Shevchenko and C. Klason, Proc. 1994 North American Conf. on Smart Structures and Materials, SPIE, 2191, 1994, 399.

- 3 F. Gubbels, R. Jérôme, Ph. Teyssié, E. Vanlathem, R. Deltour, A. Calderone, V. Parenté and J. L. Brédas, *Macromolecules*, 27 (1994) 1972.
- 4 F. Gubbels, S. Blacher, E. Vanlathem, R. Jérôme, R. Deltour, F. Brouers and Ph. Teyssié, *Macromolecules*, 28 (1995) 1559.
- 5 F. Hindryckx, P. Dubois, R. Jérôme, P. Teyssié and M. G. Marti, *J. Appl. Polym. Sci.*, 64 (1997) 423 and 439.
- 6 Y. Kamiya and E. Niki, In: *Aspects of Degradation and Stabilization of Polymers* (Ed. H. H. G. Jellinek), Elsevier, Amsterdam 1978. p. 80.
- 7 T. Atkins and C. Batich, *MRS Bulletin*, 18 (1993) 40.
- 8 W. Schnabel, *Polymer Degradation: Principles and Practical Applications*, Macmillan, New York 1981.
- 9 M. Amin and A. Maadhah, In: *Handbook of Polymer Degradation* (Ed. S. H. Hamid), Marcel Dekker, New York 1992.